https://www.scientificarchives.com/journal/journal-of-nanotechnology-and-nanomaterials

Journal of Nanotechnology and Nanomaterials Research Article

Rapid Inactivation of SARS-CoV-2 by Coupling Tungsten Trioxide (WO_3) Photocatalyst with Copper Nanoclusters

Silvia Ghezzi[1], Isabel Pagani[1], Guido Poli[2], Sudipto Pal[3], Antonio Licciulli[3], Stefano Perboni[4*], Elisa Vicenzi[1*]

[1]Viral Pathogenesis and Biosafety Unit, IRCCS San Raffaele Scientific Institute, Milan, Italy

[2]Vita-Salute San Raffaele University School of Medicine, Milan, Italy

[3]Department of Innovation Engineering, University of Salento, Via Per Monteroni, Lecce, Italy

[4]Nanohub, Milan, Italy

[*]Correspondence should be addressed to Elisa Vicenzi; vicenzi.elisa@hsr.it, Stefano Perboni; s.perboni@nanohub.it

Received date: August 14, 2020, **Accepted date:** December 02, 2020

Abstract

Severe acute respiratory syndrome coronavirus-2 (SARS-CoV-2), the etiological agent of coronavirus disease 2019 (COVID-19) is transmitted person-to-person via respiratory droplets and through smaller droplets that are light enough to form an aerosol that remain suspended in the air and contaminate the surfaces particularly in indoor conditions. Thus, effective measures are needed to prevent SARS-CoV-2 transmission in indoor environments. In this regard, we have investigated the ability of a system based on combining tungsten trioxide-based (WO_3) photocatalyst and copper nanoclusters coated fabric to inactivate SARS-CoV-2. To this purpose, an infectious SARS-CoV-2 suspension was introduced in a photocatalytic reactor containing a WO_3 coated grid and a lighting system that activates WO_3. Aliquots of fluid were collected every 10 min (up to 60 min) and tested for their infectivity by means of a viral plaque assay in Vero cells whereas, in parallel, the viral RNA content was measured by quantitative PCR (qPCR). A 1:3,400 ratio of plaque forming units (PFU) vs. viral RNA copies was observed for SARS-CoV-2. After 10 min, the infectious viral content was decreased by 98.2% reaching 100% inactivation after 30 min whereas the SARS-CoV-2 RNA load was decreased of 1.5 log10 after 30 min. Thus, despite only a partial decrease of viral RNA, SARS-CoV-2 infectivity was completely inactivated by the system in 30 min. These results support the idea that this system could be exploited to achieve SARS-CoV-2 inactivation not only for liquids but also for air purification in indoor environments.

Introduction

At the end of 2019, a novel severe respiratory disease (coronavirus disease 2019, COVID-19) spread to Wuhan, China, it became pandemic in few months, with more than 41 million people infected worldwide as of October 2020. COVID-19 is caused by a novel virus called severe acute respiratory syndrome (SARS) CoV-2 to distinguish it from SARS-CoV that emerged in Guangdong province in China in 2003 and caused the severe clinical condition known as SARS. Like SARS-CoV, SARS- CoV-2 causes a severe interstitial pneumonia that leads to acute respiratory distress syndrome (ARDS) and death [1-5].

The transmission of SARS-CoV-2 is not yet completely defined as airborne [6]. The droplets are expelled when a person speaks, particularly with a loud voice [7], coughs and sneezes [8] whereas aerosols originate from dissemination of the droplet nuclei [9]. Both droplets and aerosols have been shown to contain SARS-CoV-2 suggesting that they are a potential source of infectious virus although the virus infectivity has not been yet determined [10]. As the droplets are classically described as larger entities (>5 μm) as compared with aerosols (<5 μm), they quickly drop to the surfaces and ground by force of gravity whereas aerosols remain suspended in the air for a longer time [11]. Experimental studies have shown that the SARS-CoV-2 virions can remain infectious in aerosol for hours and on inert surfaces up to days [12]. Furthermore, during SARS-CoV pandemic in 2003, a major route of transmission was identified in aerosols generated in the sewing systems as observed in an apartment building in Hong Kong, suggesting that not only infected droplets, but also droplet nuclei, can be a source of infectious virus [13]. Furthermore,

as most of the secondary cases have been reported in indoor environments [6], device that inactivate infectious virions present in the droplets and droplet nuclei might prevent the spreading of the infection.

Virus inactivation by physical means has been extensively studied, as reviewed in [14]. Photocatalysis is the natural phenomenon by which the speed of a chemical reaction is accelerated through the action of either natural or artificial light [15]. Titanium dioxide (TiO_2) photocatalysts have been widely used in this field. The disadvantage of TiO_2 photocatalyst is that it needs to be exposed to ultraviolet (UV) light in order to be activated [16] thus causing adverse health issues. In this regard, the development of visible light active photocatalysts is highly desirable and recently tungsten trioxide (WO_3)-based photocatalysis has significantly increased the attention due to its high stability in acidic/oxidative environment and its ability to absorb the whole visible light spectrum [17]. Upon visible light exposure, WO_3 absorbs the photon that excites the valance band electron to the conduction band creating electron-hole pair, which reacts with water (air humidity) and oxygen to create hydroxyl radicals (·OH) and superoxide anions (O_2^-) [18]. Billions of these reactive oxygen intermediates (ROI) are generated which can effectively damage the membranes of bacteria, cells, and tissues [19]. The ultimate result is an effective decomposition of pathogens like viruses and bacteria and organic and inorganic pollutants, nitrogen oxides, poly-condensed aromatics, sulfur dioxide, carbon monoxide, formaldehyde, methanol, ethanol, benzene, ethylbenzene and other volatile organic compounds (VOCs) [20]. The strong oxidative effect of WO_3 provides the rationale to explore it as a disinfectant of air and solid surfaces. Although many studies have been reported on photocatalytic inactivation of bacteria, only a few studies have addressed virus inactivation [21]. Another pathogen killer is copper and its compounds which have been used as disinfectant, antimicrobial and antiviral agent for many years [22-24]. By combining the two processes in one system, a superior efficiency of virus inactivation is expected.

Many studies have shown that copper surfaces can release ions that cause oxidative stress by producing reactive oxygen species (ROS) [25]. Copper coated filters can therefore inactivate viruses by contact killing mechanism while the virus containing fluids passes through the device [26]. As antiviral and antibacterial mechanism of copper is well known and documented, the copper nanoparticles (CuNPs) coated fabric was kept inside the filtration system. The antiviral activity should take place where the copper ions are released from the copper surface. Copper could easily oxidize in presence of humidity and air, especially when it comes to submicron sizes.

On these premises, we have evaluated the combination of WO_3 based photocatalyst system and copper coated fluid filters to interfere with SARS-CoV-2 infectivity.

Materials and Methods

Photocatalysis system

The photocatalytic system used in this study is in liquid phase and relies on the combination of two elements: a metallic mesh filter coated with WO_3 nanoclusters and a cotton fabric treated with metallic CuNPs. To prepare the CuNPs coated fabric, a wet chemical synthesis process was used following the modified process described by Zhou et al. [24]. Briefly, Cu nanoclusters were first synthesized in the aqueous media from Cu cations dissolved from copper acetate monohydrate salt (98%, Sigma-Aldrich) and hydrazine hydrate (80% solution in water, Sigma-Aldrich) as the reducing agent. All reagents were ACS grade. Cations were reduced and clustered in the aqueous medium. The fabric was immersed in the nanocluster suspension for 6-8 hours. The metal nanoparticles spontaneously deposit on to the fabric threads by attraction of the hydroxyl groups present on the cotton-based fabric (coming from the cellulose part of the fabric). The dispersion efficiency is evaluated in terms of weight gain due to the copper deposition on the fabric. The integrity of the layer of CuNPs deposited on the fibers and WO_3 nanoclusters were analyzed by scanning electron microscopy (SEM) by using a ZEISS EVO 4°C VP microscope.

SARS-CoV-2 plaque assay

The SARS-CoV-2 stock (GISAID accession ID: EPI_ISL_413489) was diluted 1:100 to obtain 80 ml of viral suspension with an infectious titer of $1.7x10^4$ plaque forming units (PFU)/ml. The viral suspension was introduced into the device from its top and aliquots were collected at the bottom every 10 min up to 60 min. The collected viral suspension was then tested for the presence of infectious virus as determined by a previously optimized plaque assay on Vero cells [27] and quantification of viral RNA by real-time PCR, described below.

Vero cells were seeded at $1.5x10^6$ cell/well in 6-well plates in Eagle's Minimum Essential Medium (EMEM) supplemented with 10% fetal calf serum (complete medium). After 24 h, 1:10 serial dilutions of the virus containing suspensions were collected at various time intervals after processing through the device and were incubated with Vero cells for 60 min. Cell supernatants were then discarded and 1% methylcellulose (1.5 ml/well) dissolved in complete medium was added to each well. After 3 days, cells were fixed with formaldehyde/PBS solution (6%) and stained with crystal violet (1%; Sigma

Chemical Corp.) in 70% methanol. Viral plaques were counted under a stereoscopic microscope (SMZ-1500, Nikon) according to the previous article [28]. Viral titers were expressed as PFU/ml.

SARS-CoV-2 quantitative PCR

Viral RNA was extracted from the viral suspension collected at different time intervals after processing through the device. Viral RNA was extracted by using QIAamp Viral RNA Mini Kit (Qiagen). Real-time quantitative PCR (qPCR) for the nucleocapsid (N) gene was performed to determine the viral RNA copies present after inactivation. The viral RNA quantification was carried out with the Quanty COVID-19 Kit (Clonit, Milan, Italy) that includes a reference curve of viral RNA at known copy number with a 7500 Fast Real-Time PCR System (Applied Biosystems).

Statistical analysis

Prism GraphPad software v. 8.0 (www.graphpad.com) was used for all statistical analyses. Comparison among groups were performed using the one-way analysis of variance (ANOVA) and the Bonferroni's multiple comparison test. Comparison between two homogenous groups was performed by a paired t-test.

Results and Discussion

The distribution of WO_3 nanocluster coated on the metallic mesh filter is shown in Figure 1. The particles were well sticked and homogeneously distributed on the surface of the metallic mesh filter. The particle size had a medium size of 25 nm. The morphology of copper coated fibers is shown in Figure 2. The average particle size of copper nanoparticles is in the range of 300 nm (Figure 2A). Agglomeration of individual CuNPs takes place randomly during the deposition process as shown in Figure 2B.

To evaluate SARS-CoV-2 inactivation, the virus inoculum was introduced in the photocatalytic reactor containing the WO_3/CuNPs filter and the light-based system that activates WO_3 and aliquots of the viral suspension were collected after 10 min and continued up to 30 min. As shown in Figure 3, the kinetic of infectious virus, as expressed in PFU/ml, indicates that, after 10 min, the WO3 device inactivated SARS-CoV-2 infectious titers by 98.2% and reached 100% inactivation after 30 min.

The amount of viral RNA by qPCR was evaluated; as shown in Figure 4A, the levels of viral RNA in the inoculum were ca. 3,400-fold higher than the infectious titers measured in PFU/ml consistently with previous observations with

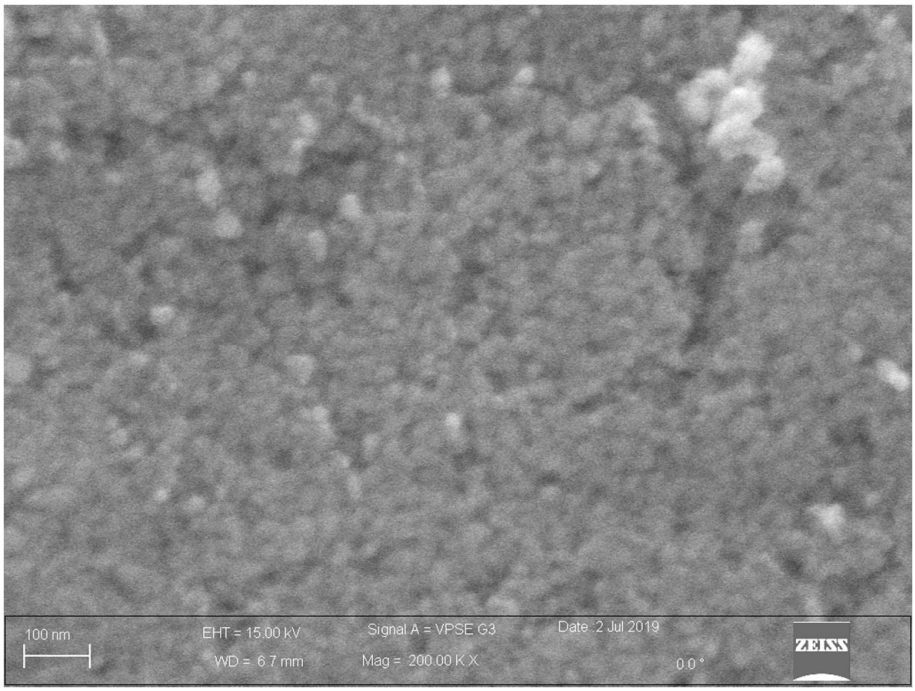

Figure 1: Field emission scanning electron microscopic (FESEM) image of the WO3 nanoclusters coated on the wire mesh showing homogeneous distribution of the WO3 nanoparticles on the surface of the metallic mesh filter. The particle size was approximately 25 nm.

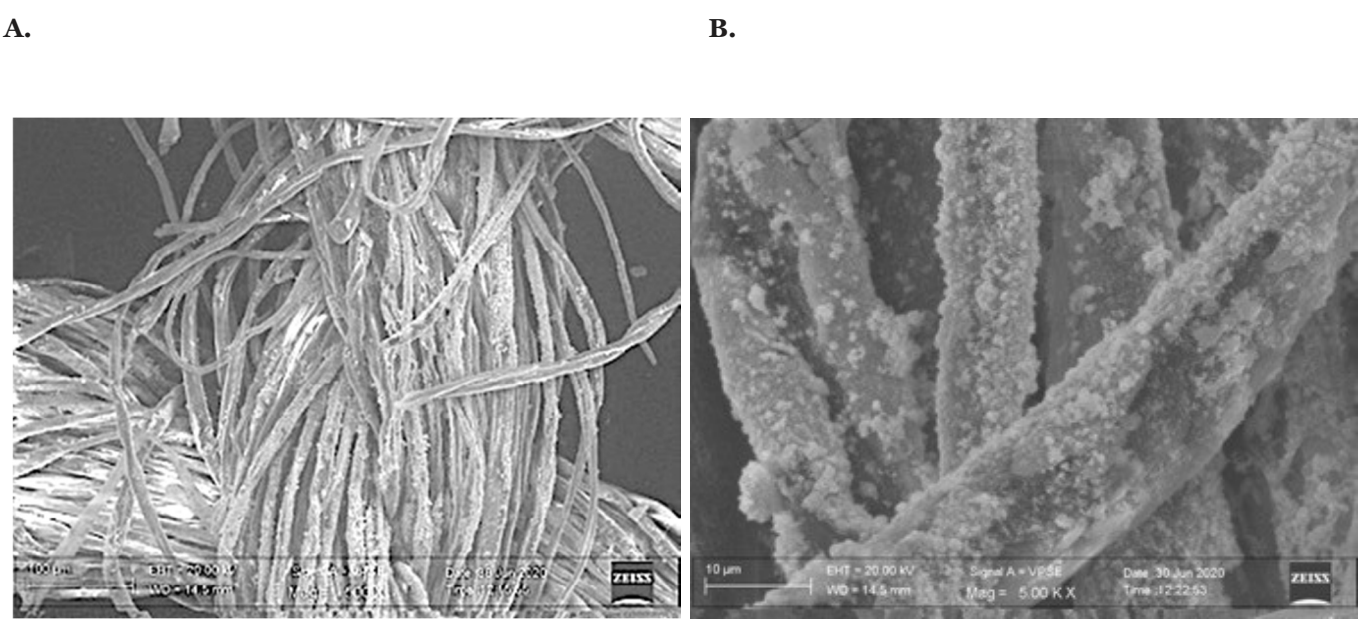

Figure 2: SEM images of the Cu nanocluster coated fabric; A. All single fibers of the fabric thread are coated with the CuNPs. The particles of copper are estimated to be 300 nm in size; B. Magnified image of the clusters of CuNPs that are strongly adherent to the fabric.

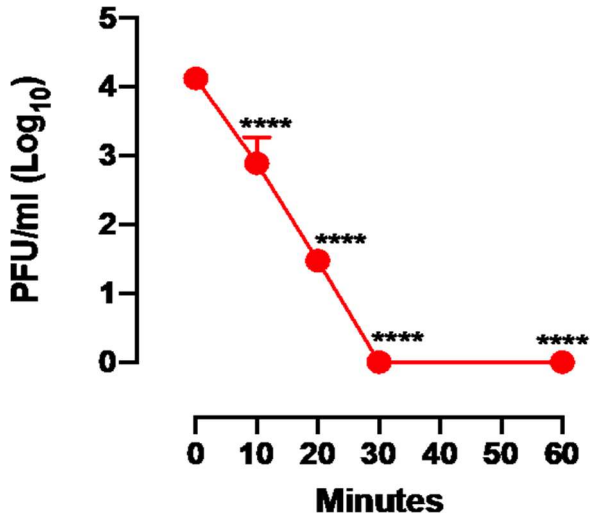

Figure 3: Kinetic of SARS-CoV-2 infectivity inactivation by WO_3 treatment. Viral titers were determined by a plaque assay in Vero cells prior to introduction of the SARS-CoV2 into the device and after 10 min of treatment up to 60 minutes. Mean values of three independent experiments are shown. ****indicate a p value <0.0001 as determined by one-way ANOVA with Bonferroni's correction.

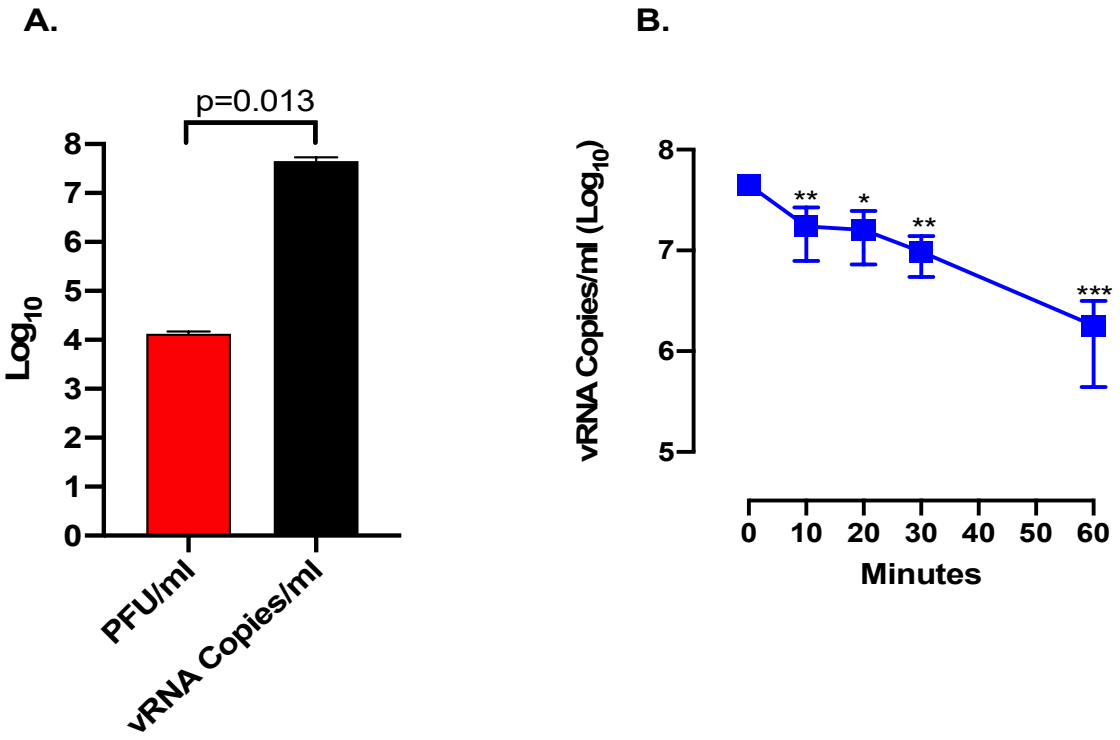

Figure 4: Kinetic of SARS-CoV-2 RNA inactivation by WO_3 treatment; A. Titer of input virus as determined by the plaque assay (red bar) and qPCR (black bar); B. Kinetic of viral RNA inactivation by WO_3 treatment as determined by qPCR. *indicates a p value <0.05, **indicate a p value <0.01 as determined by one-way ANOVA with Bonferroni's correction.

SARS-CoV [28]. Indeed, the WO_3/CuNPs inactivation system progressively and significantly reduced the amount of detectable viral RNA (Figure 4B), although not as efficiently as in the case of PFU inactivation.

The WO_3 photocatalyst generates a large number of ROI that react very rapidly and efficiently with proteins, lipids and nucleic acids [29]. The destruction of viral proteins, particularly the spike protein that protrudes out of the envelope and the other envelope proteins (i.e. envelope (E) and membrane (M)) likely explains the rapid inactivation of SARS- CoV-2 infectivity. It is tentative to speculate that the generated ROI damage the virion envelope causing the release of genomic RNA, the internal component of viral particles. However, this phenomenon is less efficient than the destruction of the viral protein as genomic RNA is well preserved inside the virion packaged by the tightly bound nucleocapsid protein that likely exerts a shield effect [30].

In comparison to other systems, such as those based on UV light [31], this system has the advantage to be used safely in the presence of people. All reactions (e.g. virus inactivation and disintegration of other substances) take place in the filter without the release of substances that could be potential hazardous to human and animal health. Furthermore, this system has minimum maintenance requirements and low electricity consumption. The test was carried out in liquid through SARS-CoV-2 contact with the photocatalytic filter and antiviral tissue. It is expected that similar results would be obtained with an air treatment device that uses the same filtration system in indoor environments.

In conclusion, combination of photocatalytic and copper disinfection has the potential to significantly reduce SARS-CoV-2 titer in liquid and in air and, consequently, the contamination of surfaces. The system might contribute to a more general containment of the pandemic in synergy with social distancing and individual measures of protection and hygiene. Our study supports the hypothesis that a technological device could be used for the inactivation of infectious SARS-CoV-2, and potentially of other viruses, from the air particularly in indoor environments.

References

1. Guan WJ, Zhong NS. Clinical Characteristics of Covid-19 in China. Reply. The New England Journal of Medicine. 2020 Mar 27;382.

2. Wölfel R, Corman VM, Guggemos W, Seilmaier M, Zange S, Müller MA, et al. Virological assessment of hospitalized patients with COVID-2019. Nature. 2020 May;581(7809):465-9.

3. Zou L, Ruan F, Huang M, Liang L, Huang H, Hong Z, et al. SARS-CoV-2 viral load in upper respiratory specimens of infected patients. New England Journal of Medicine. 2020 Mar 19;382(12):1177-9.

4. Liu Y, Yan LM, Wan L, Xiang TX, Le A, Liu JM, et al. Viral dynamics in mild and severe cases of COVID-19. The Lancet Infectious Diseases. 2020 Mar 19.

5. Lavezzo E, Franchin E, Ciavarella C, Cuomo-Dannenburg G, Barzon L, Del Vecchio C, et al. Suppression of a SARS-CoV-2 outbreak in the Italian municipality of Vo'. Nature. 2020 Aug;584(7821):425-9.

6. Klompas M, Baker MA, Rhee C. Airborne transmission of SARS-CoV-2: theoretical considerations and available evidence. JAMA. 2020 Aug 4.

7. Asadi S, Wexler AS, Cappa CD, Barreda S, Bouvier NM, Ristenpart WD. Aerosol emission and superemission during human speech increase with voice loudness. Scientific Reports. 2019 Feb 20;9(1):1-0.

8. Scharfman BE, Techet AH, Bush JW, Bourouiba L. Visualization of sneeze ejecta: steps of fluid fragmentation leading to respiratory droplets. Experiments in Fluids. 2016 Feb 1;57(2):24.

9. Chao CY, Wan MP, Morawska L, Johnson GR, Ristovski ZD, Hargreaves M, et al. Characterization of expiration air jets and droplet size distributions immediately at the mouth opening. Journal of Aerosol Science. 2009 Feb 1;40(2):122-33.

10. Liu Y, Ning Z, Chen Y, Guo M, Liu Y, Gali NK, et al. Aerodynamic analysis of SARS-CoV-2 in two Wuhan hospitals. Nature. 2020 Jun;582(7813):557-60.

11. Jayaweera M, Perera H, Gunawardana B, Manatunge J. Transmission of COVID-19 virus by droplets and aerosols: A critical review on the unresolved dichotomy. Environmental Research. 2020 Jun 13:109819.

12. Van Doremalen N, Bushmaker T, Morris DH, Holbrook MG, Gamble A, Williamson BN, et.al. Aerosol and surface stability of SARS-CoV-2 as compared with SARS-CoV-1. New England Journal of Medicine. 2020 Apr 16;382(16):1564-7.

13. Yu IT, Li Y, Wong TW, Tam W, Chan AT, Lee JH, et al. Evidence of airborne transmission of the severe acute respiratory syndrome virus. New England Journal of Medicine. 2004 Apr 22;350(17):1731-9.

14. Zhang C, Li Y, Shuai D, Shen Y, Xiong W, Wang L. Graphitic carbon nitride (g-C3N4)-based photocatalysts for water disinfection and microbial control: A review. Chemosphere. 2019 Jan 1;214:462-79.

15. Ren H, Koshy P, Chen WF, Qi S, Sorrell CC. Photocatalytic materials and technologies for air purification. Journal of Hazardous Materials. 2017 Mar 5;325:340-66.

16. Foster HA, Ditta IB, Varghese S, Steele A. Photocatalytic disinfection using titanium dioxide: spectrum and mechanism of antimicrobial activity. Applied Microbiology and Biotechnology. 2011 Jun 1;90(6):1847-68.

17. Nguyen TT, Nam SN, Son J, Oh J. Tungsten Trioxide (WO3)-assisted Photocatalytic Degradation of Amoxicillin by Simulated Solar Irradiation. Scientific Reports. 2019 Jun 27;9(1):1-8.

18. Shi X, Siahrostami S, Li GL, Zhang Y, Chakthranont P, Studt F, et al. Understanding activity trends in electrochemical water oxidation to form hydrogen peroxide. Nature Communications. 2017 Sep 26;8(1):1-6.

19. Vatansever F, de Melo WC, Avci P, Vecchio D, Sadasivam M, Gupta A, et al. Antimicrobial strategies centered around reactive oxygen species–bactericidal antibiotics, photodynamic therapy, and beyond. FEMS Microbiology Reviews. 2013 Nov 1;37(6):955-89.

20. Nosaka Y, Nosaka AY. Generation and detection of reactive oxygen species in photocatalysis. Chemical Reviews. 2017 Sep 13;117(17):11302-36.

21. Matharu RK, Ciric L, Ren G, Edirisinghe M. Comparative Study of the Antimicrobial Effects of Tungsten Nanoparticles and Tungsten Nanocomposite Fibres on Hospital Acquired Bacterial and Viral Pathogens. Nanomaterials. 2020 Jun;10(6):1017.

22. Alshabander BM. Copper (II)-doped WO3 nanoparticles with visible light photocatalytic antibacterial activity against gram-positive and gram-negative bacteria. Inorganic and Nano-Metal Chemistry. 2020 Apr 22:1-5.

23. Yamauchi K, Ochiai T, Yamauchi G. The Synergistic Antibacterial Performance of a Cu/WO 3-Added PTFE Particulate Superhydrophobic Composite Material.

Journal of Biomaterials and Nanobiotechnology. 2015 Jan 6;6(01):1.

24. Zhou H, Zhang T, Yue X, Peng Y, Qiu F, Yang D. Fabrication of flexible and superhydrophobic melamine sponge with aligned copper nanoparticle coating for self-cleaning and dual thermal management properties. Industrial & Engineering Chemistry Research. 2019 Mar 4;58(12):4844-52.

25. Vincent M, Duval RE, Hartemann P, Engels-Deutsch M. Contact killing and antimicrobial properties of copper. Journal of Applied Microbiology. 2018 May;124(5):1032-46.

26. Szekeres GP, Németh Z, Schrantz K, Németh K, Schabikowski M, Traber J, et al. Copper-coated cellulose-based water filters for virus retention. ACS Omega. 2018 Jan 31;3(1):446-54.

27. Pagani I, Ghezzi S, Ulisse A, Rubio A, Turrini F, Garavaglia E, et al. Human endometrial stromal cells are highly permissive to productive infection by Zika virus. Scientific Reports. 2017 Mar 10;7:44286.

28. Pacciarini F, Ghezzi S, Canducci F, Sims A, Sampaolo M, Ferioli E, et al. Persistent replication of severe acute respiratory syndrome coronavirus in human tubular kidney cells selects for adaptive mutations in the membrane protein. Journal of Virology. 2008 Jun 1;82(11):5137-44.

29. Adhikari S, Sarkar D, Madras G. Highly efficient WO3–ZnO mixed oxides for photocatalysis. RSC advances. 2015;5(16):11895-904.

30. Chang CK, Hou MH, Chang CF, Hsiao CD, Huang TH. The SARS coronavirus nucleocapsid protein–forms and functions. Antiviral Research. 2014 Mar 1;103:39-50.

31. Hajkova P, Spatenka P, Horsky J, Horska I, Kolouch A. Photocatalytic effect of TiO2 films on viruses and bacteria. Plasma Processes and Polymers. 2007 Apr;4(S1):S397-401.